PAPER • OPEN ACCESS

Design of bio-inspired muscle sarcomere structure using a hybrid hydrogel-IPMC actuator

To cite this article: H M Hamdi *et al* 2020 *IOP Conf. Ser.: Mater. Sci. Eng.* **973** 012043

View the article online for updates and enhancements.

Design of bio-inspired muscle sarcomere structure using a hybrid hydrogel-IPMC actuator

H M Hamdi[1], SAAbdelwahhab[2], MIAwad[3] and FATolbah[3]

[1] Design and Production Engineering Department, Faculty of Engineering, Ain Shams University, Cairo, Egypt.
[2] Production Technology Department, Faculty of Industrial Education, Helwan University, Cairo, Egypt.
[3] Mechatronics Engineering Department, Faculty of Engineering, Ain Shams University, Cairo, Egypt.

hend.hamdi@eng.asu.edu.eg

Abstract. Biological muscle is considered a powerful actuator due to its flexibility, lightweight, and efficiency. The building unit of a muscle, sarcomere, and the study of its energy balance cycle is considered in researches due to its importance to mimic the micro-level muscle structure to improve the artificial muscle performance. In this work, a new design of a linear actuator based on the sarcomere behavior is developed. The design is inspired by studying the four steps adenosine triphosphate (ATP) hydrolysis cycle, which is the main source of the required energy for sarcomere contraction. A new developed hybrid hydrogel-polymeric material actuator is designed in this paper using a combination between Ionic Polymeric Metallic Composites (IPMC) and hydrogel to behave like the sarcomere. This new actuator proposes an autonomous cycle using the effect oscillatory Belousov–Zhabotinsky (BZ) reaction. The physical model is proposed, and the mathematical model of the actuator is derived and formulated and identified using MATLAB/ Simulink.

1. Introduction

Bioinspired actuators have been recently intensified to cover many fields, as the continuous improvement of automated systems requires efficient energy utilization [1], where the conventional actuators have weakness in force to weight ratio [2], [3]. The natural muscle is considered an important source of inspiration for its multi-tasking motion, flexible design, and efficient energy utilization. [2].Natural muscle has many models such as Hill model, in which the muscle is studied as three element mechanical system, and Huxley model, in which the muscle is studied on the micro level and the main building unit- sarcomere- behavior is considered. The previously mentioned models are widely used, and it was found that studying the muscle behaviour on the micro-level, and simulating the sarcomere behavior gives better and smoother results, so this study focuses on Huxley's model. Then it is required to understand the four-states Adenosine Tri Phosphate (ATP) chemical cycle, which is the actuating sarcomere contraction cycle.

The evolution of Electro Active Polymers (EAP) helps to fulfil the bioinspired actuators designs. They give a large mechanical response as stretching, bending, buckling, and volumetric change under the effect of many types of physical stimulators [4]. EAP is divided into two main types, electronic and ionic. Ionic Polymeric Metal Composites (IPMC) is a class of ionic polymers [5], which exerts a

large bending value when excited by a low electric voltage. This privilege was utilized in [6] to simulate the muscle protein motion in the sarcomere. This design is extended in this work adding a chemically stimulated hydrogel terminal that can shrink, expand, and move to different binding sites. The proposed hybrid material actuator simulatesthe four-state ATP actuation cycle of the sarcomere.

2. Artificial Muscles and Their Materials

2.1 Natural Muscle Contraction Cycle

Natural skeletal muscle is responsible for motion control. It is responsible for maintaining bones and joints stability and prevents excessive movements which may cause damage or deformation[7].The sarcomere is the main actuating unit of striated muscle. It is important to study its construction and its contraction mechanism to understand the muscle behaviour.

The striated muscle consists of myofibrils shown in figure 1 (a). It consists of periodically repeated structures called sarcomeres. Each sarcomere consists of coiled protein filaments, the thin chain called actin and the thick one called myosin. Which are the main motive elements of the muscle contraction [8].

The study of the energy balance of muscle contraction cycle needs to go through the micro level of muscle and brief description of actin-myosin cycle of the sarcomere. It was proven that the trajectories of force and muscle length along time were smoother and more relevant. Studies shows that the microscopic level of modeling is more appropriate[9].

The muscle contraction cycle is directly related to the ATP hydrolysis cycle which is the main source of the required energy. In the absence of calcium, there is no activities done by any of both sarcomere motor proteins, actin and myosin. As Ca++ binds the actin sites, the cycle starts. The ATP cycle was first illustrated by Lymn and Taylor as follows:

$$ATP \rightleftharpoons ADP + Pi + energy \qquad (1)$$

where ADP is the responsible for myosin head attachment to the actin and cross bridge formation. The resulting energy causes the pull the actin to move forward[10].Then, the ATP hydrolysis enables the myosin head to start the power-stroke, causes the slipping between the actin filaments and myosin head.[11].

The one- direction myosin head movement from a binding site along the actin to another is divided into 4 main steps:Disengagement between actin and myosin and a new ATP molecule arrives, preparing for the new step forward which called recovery stroke, Engagement between actin an myosin at the actin binding sites, The myosin head moves forward pulling the actin filament using the released energy coming from ATP hydrolysis[12]. The coupling between the mechanical and chemical cycles of the motor proteins is illustrated in figure 2, showing the power and return stroke synchronized with the ATP hydrolysis[13].
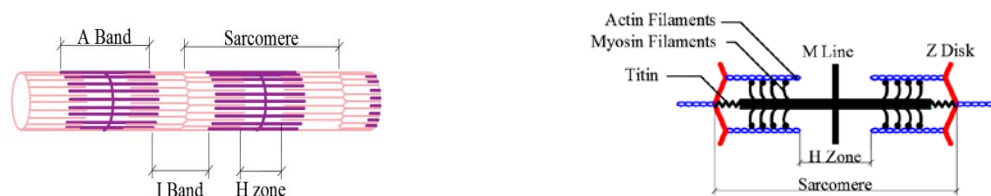
(a) The myofibril configuration and the action zones during   (b) A single sarcomere unit.

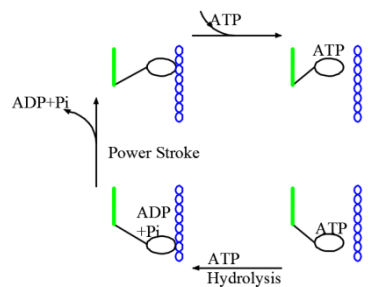**Figure 1.** Natural Sarcomere Details.

Figure 2. The coupling between the mechanical and chemical states during the ATP hydrolysis 4 steps cycle.

All the previous work agreed with the presence of four mechanical states resulting from the ATP hydrolysis reaction. Here we will focus on the actuation cycle of the sarcomere. The objective of this work is to propose a new sarcomere-like actuator simulating the previously mentioned four sates cycle of the muscle contraction in order to be simulated, aiming to optimize the energy required to perform the cycle.

2.2 Artificial Muscles Designs and Materials

Artificial muscles are widely used in the bio-robots field. Many designs were developed to resemble thenatural muscle behavior efficiently. The mechanical motors and pneumatic and hydraulic systems early designs of those biomimetic actuators but the large size and the need of hydraulic pumps caused low system efficiency regarding to size [15] [16].

Although there are many types of biomimetic actuators were invented to act as the natural muscle, electroactive polymers (EAP) were found to be the closest type to the actual performance, since they have close range of actuation force, same nature in deflection, and suitable mechanical work cycle needed to give the required chemical cycle steps [2]. They are superior to SMA because they have lower density and higher response and resilience. The two basic classes are electronic EAP and ionic EAP, the second is preferred duo to lower required activation voltage and higher resultant displacement. Hybrid material actuator is proposed in [17] to behave like myosin unit during power stroke and return, since the behaviour of each material results in different deflection under activation.
 In current research, the designs in [6] and [17] are incorporated to propose a hybrid bio-inspired four states cycle actuator that can attach a sequence of binding sites. The IPMC is electrically actuated and acts as myosin lever arm, and attached with a chemically actuated hydrogel terminal which acts as myosin head. The self-oscillating chemical reaction enables the actuation cycle to be repeated to perform muscle like contraction.

2.3 Hydrogels and Swelling Reaction

Hydrogels are elastic materials that have increasing volume (or swelling) if it is actuated by stimulus, which can be chemical, electrical, magnetic, or thermal, which makes them suitable to be used in biomimetic actuators design. Chemically stimulated gels- even by oscillating reaction or varying pH- give more powerful results rather than using electrical stimulation [14].It is performed by immersing gel into water or solvent or changing the chemical environment, which results in cation and anion exchange [15]. The oscillatory Belousov–Zhabotinsky (BZ) reaction was utilized by Yoshida in [16] is one of the chemical stimulation methods for the hydrogels, generating an autonomous cycling of oxidation and reduction needed for hydrogel swelling. It possesses better performance than the pH stimulation since it doesn't need any external control for the surrounding reactors needed to change the solution status[17]. This internal stimulation cyclic was applied to propose a chemo-mechanical actuator using the effect of generated chemical wave inside the gel to provide motion. Further, the generated osmosis pressure of this propagated wave was used to actuate a chemical robot that can provide motion to an object [18].

The beating behavior of the gel is due to the existing metal ions- ruthenium Ru- in the polymer network working as a catalyst. The gel swells while Ru oxidation (Rubpy3) and de-swells while the reduction (Rubpy2). This repeating cycle which is driven by the BZ reaction provides autonomous controllable motion as a kind of chemical energy transformation to mechanical energy used in biorobots design [19].

The abovementioned behavior is utilized in the developed actuator as a beating head generates an autonomous voltage signal. This voltage signal results in cyclic IPMC strip bending. The beating gel head turn on the operating switch while swelling and the switch is turned off while deswelling.

2.4 Ionic Polymeric Metallic Composites (IPMC's)

IPMC's are commonly used in the field of soft actuator because of their ability to transform electrical energy into mechanical energy in a form of strip bending when the electric filed is applied. Further, it shows a relatively large bending displacement under the effect of low voltage[20]. It consists of Nafion membrane, plated with two electrodes on each side [21].

The shape of IPMC is a polymeric cantilever membrane contains fixed anions on the polymer chain, free cations, and water molecules. When a voltage is applied as shown in figure 4, the hydrated cations are attached to the negative electrode side, causes osmosis pressure results in overall membrane deformation, mainly bending displacement [22], [23].
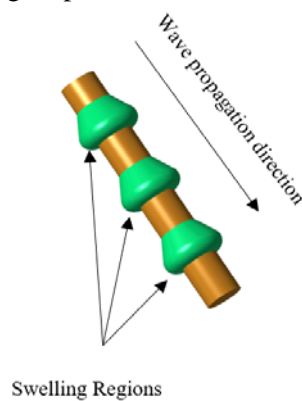

Figure 3. The chemical wave generated by the BZ reaction and the resulting swelling shape in the hydrogel.
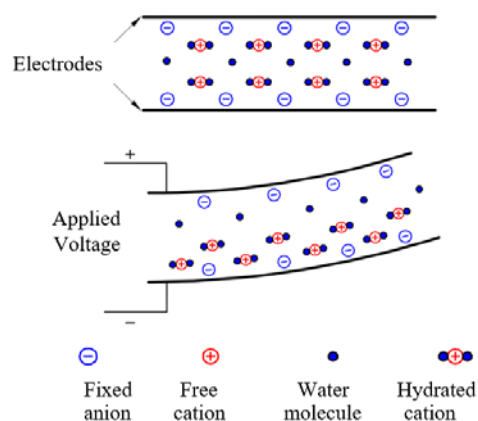

Figure 4. The effect of electrical activation of the IPMC membrane by applying voltage on the surface electrode and the resulting bending.

This previously described electromechanical behavior of the IPMC material was analyzed to determine the cantilever tip displacement and resultant force needed for actuation. The applied voltage on the IPMC strip is due to the hydrogel head expansion which results in sequence of pulses with

variable duration controlled by changing the initial concentration of the acids as escribed in the following section.

3. Proposed Sarcomere-Like Actuator Mechanical Model

The presented actuator is a new sarcomere-like actuator simulating the previously mentioned four sates cycle of the muscle contraction. The proposed actuator is adopted from [6]. The design is extended to fulfil the proposed autonomous cyclic motion requirements by adding a hydrogel terminal as an actuator head. The gel terminal is affected by the cyclic oxidation-reduction resulting from the Belousov–Zhabotinsky (BZ) reaction, and the wave propagates along its edge. The operating sequence of the actuator is presented in figure 5.

The main actuating element of the proposed actuator is an IPMC strip ended with a cyclic swelling hydrogel head, which controls an on-off switch during swelling-deswelling cycle. The switching point is located inside the slider so that it is in contact with the gel wave at the middle of the cycle as illustrated in figure 6 enabling it to go forward and return by strip bending as a result of electrical activation of the bottom electrodes. The gel heads are loosely positioned into a slider slots, supplied with the acidic solution.

At the period of contact between the gel wave region and the slider connection point, an electric voltage signal is given to the electrode attached to the IPMC strip terminal, which starts bending in turn. When the wave travels away from the switching point, the voltage signal is removed letting the IPMC flapper strip to return to the idle position. Since the gel head is attached to the slider, it performs forward stroke during bending and then it stays at the new position. During the return stroke the gel head is loose and the IPMC strip returns to initial position. This cycle can be repeated enabling the slider to move steps forward instead of on-off movement and fluctuating between two points.
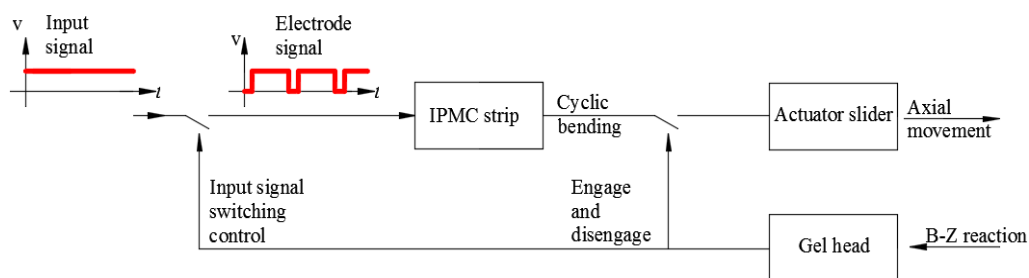

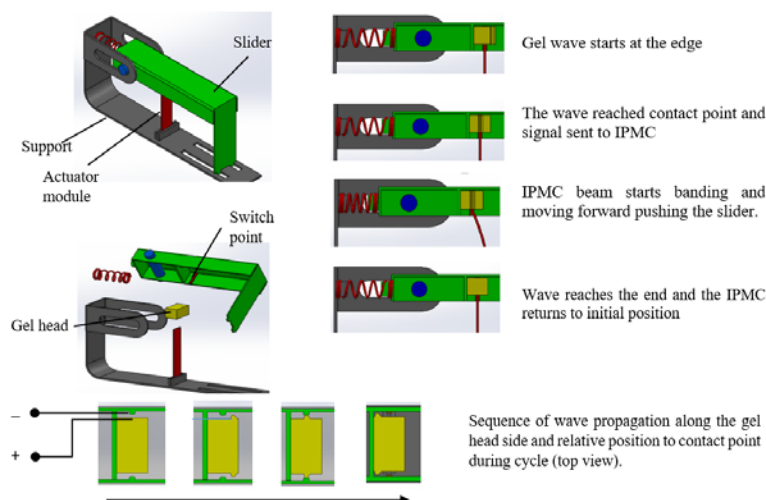**Figure 5.** The operating sequence of the proposed hybrid material actuator.

Figure 6. The proposed actuator mechanical model.

4. Mathematical Modeling

4.1   Modeling of Hydrogel Head Swelling Wave

The mathematical model of the BZ chemical reaction is presented in the following equations (2) to (4).

$$\frac{du}{dt} = F(u, v, \phi) \tag{2}$$

$$\frac{dv}{dt} = G(u, v, \phi) \tag{3}$$

$$F(u, v, \phi) = (1 - \phi)^2 u - u^2 - (1 - \phi)fv[u - q(1 - \phi)^2/u + q(1 - \phi)^2] \tag{4}$$

$$G(u, v, \phi) = \varepsilon[(1 - \phi)^2 u - (1 - \phi)v] \tag{5}$$

where u is the stimulus component (HBrO$_3$), v is the oxidized ion of the metal in polymer chain (Ru^{3+}), , F, G are the functions of reactants rate, f,q and $\varepsilon$are dimensionless reaction parameters, and $\phi$is the resultant volumetric fraction which is responsible of swelling and deswelling [24][19].The resulting increase in gel volumetric fraction causes the head width to expand and then increase in length. This gel swelling travelling wave can be modelled as a sine wave mentioned in equation (8) to describe the change in length with time and position [16].

$$Z_{ox}(x, t) = cos^2 \pi (x - t) \tag{6}$$

This function is dependent on wave periodic time and wavelength, it can be described by the following dimensionless mathematical presentation:

$$1 = 2 \int_0^1 Z_{ox}(x, t)dx = 2 \int_0^1 Z_{ox}(x, t)dt \tag{7}$$

Assuming there is no residual gel length at the edge, the resulting gel mechanical wave can be modelled as follows;

$$L(t) = 2 \int_0^{l_o} Z_{ox}(x, t)dx \tag{8}$$

where l_o is the average value of gel length can be calculated as follows;

$$l_o = \int_0^1 L(t)dt \tag{9}$$

The resultant wave propagation surface along the gel head edge and the resultant start and end times for the input voltage signal will be discussed in section 5.

4.2   Electromechanical Model of IPMC:

The mathematical model of the IPMC is derived from its electromechanical nature. The electrical part of the model considers the IPMC as series of$R$-C elements, as it can store discharge[25].When the electrical activation is started by the input voltage, a discharge rate is created depends on the electrical impedance of the connected layers. Figure 7 shows the electrical IPMC model, where R represents the actuator membrane DC resistance, R_i and C_i represent the ith resistance and capacitance of the electrode element i respectively [26]. These circuit elements values estimation is evaluated according to physical considerations based on IPMC geometry as follows;

$$R_i = 2\rho_i b/Lw, \quad C_i = \varepsilon_i Lw/2b \tag{10}$$

where ρ_i is electric the resistivity of segment I material, $\varepsilon_i$is electric permittivity of element i,L,w and b are the segment length, width and thickness.

To determine the discharge $Q(t)$, produced by the input voltage $v(t)$, the generalized equation of the electrical model is formed according to Kirchhoff's current law at segment i loop;

$$C_i v_i = \frac{v_i - v_{i+1}}{R_{i+1}} - \frac{v_{i+1} - v_{i+2}}{R_{i+2}} \tag{11}$$
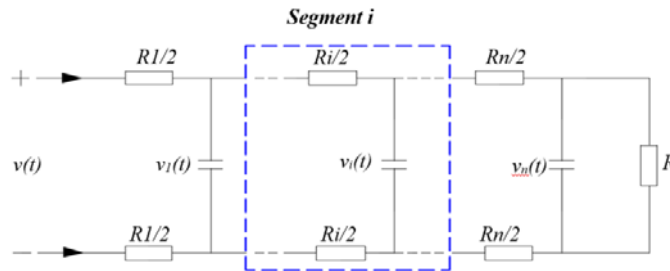

Figure 7. The electrical R-C circuit model of the IPMC.

When this model has low frequency working conditions, it is convenient to reduce the model complexity and consider the number of elements n=2 [27]. Then, relation between the input voltage *v(t)* and the absorbed current *i(t)* can be modelled in the Laplace domain as follows;

$$\frac{I(s)}{V(s)} = \frac{as^2 + bs + 1}{cs^2 + ds + e} \tag{12}$$

Then, the discharge can be estimated from the transfer function;

$$\frac{Q(s)}{V(s)} = \frac{as + b}{cs^2 + ds + e} \tag{13}$$

where,

$$a = RR_2 C_1 C_2$$
$$b = RC_1 + R_2 C_1 + RC_2$$
$$c = RR_1 R_2 C_1 C_2 \tag{14}$$
$$d = R_1 R_2 C_1 + RR_1 C_1 + RR_1 C_2 + RR_2 C_2$$
$$e = R + R_1 + R_2$$

This discharge causes a stress distribution across the cross section of the IPMC beam, which in turns crates a banding moment. The IPMC beam deflects, figure 8 due to bending moment applied and its moves forward with a displacement δ[28].

The beam bending displacement δ with no load results from the rearrangement of water molecule inside the beam- is determined by equation (15),

$$\delta(t) = k_v W(t) = 4k_v Q_i(t) \tag{15}$$

where k_v is deformation coefficient, $W(t)$ is water molecules concentrations[29].
Then we take the Laplace transformation for equation (15) and get,
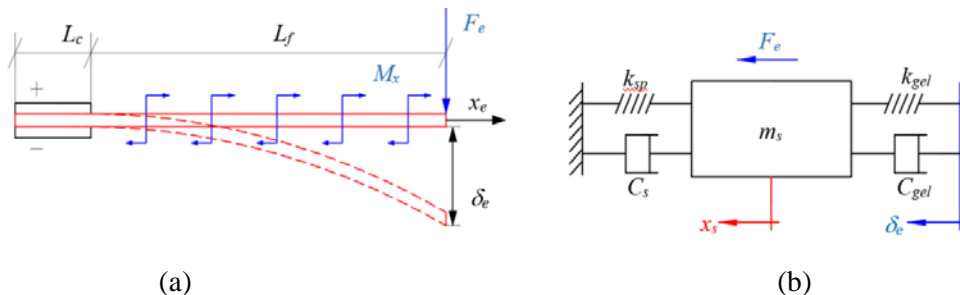
$$\delta(s) = k_v W(s) = 4k_v Q_i(s) \tag{16}$$

(a)   (b)

Figure 8. Motion analysis of the mechanical elements (a) IPMC strip (b) Slider.

Substitute from (13) into (16) we get,

$$\delta(s) = 4k_v \frac{as+b}{cs^2+ds+e} V_i(s) \tag{17}$$

To estimate the IPMC tip force, the relationship between the tip deflection δ_x and distributed moment generated along the strip M_x is given by;

$$\delta_x(t) = M_x(t).x(l_f - \frac{x}{2})/EI \tag{18}$$

So, the total induced bending moment $M_l(t)$ is given by;

$$M_l(t) = \int M_x(t)dx = F_e(t).L_f \tag{19}$$

Then the tip force $F_e(t)$ can be estimated as follows;

$$\delta(t) = \int \frac{M_l(t).l_f^2}{2EI} dt = \frac{F_e(t).l_f^3}{3EI} \tag{20}$$

$$\delta(s) = \frac{M(s).l_f^2}{2EIs} = \frac{F_e(s).L_f^3}{3EI} \tag{21}$$

Then, F_e canbe calculated as follows;

$$F_e(s) = \frac{3EI}{L_f^3} \delta(s) \tag{22}$$

As the slider connected to the IPMC beam end, considering the tip force as an input to the slider, then the slider equation of motion can be formulated as follows;

$$\dot{x} = Ax + Bu, y = Cx + Du \tag{23}$$

where x is the state vector, y is the output slider motion x_s, $A = \begin{bmatrix} 0 & 1 \\ -\frac{k_{eq}}{m_s} & -\frac{D_{eq}}{m_s} \end{bmatrix}$, $B = \begin{bmatrix} 0 \\ 1 \end{bmatrix}$, C=[1 0],

D=1, $u = F_e$, m_s is the slider mass, k_{eq} is the spring stiffness, D_{eq} is the damping coefficient due to sliding along the support guideways.

5. Simulation and Results

In order to analyse the proposed actuator performance, the wave propagation behavior is analysed to calculate the voltage activation and deactivation time. Times of start and end of voltage signal determines the duration of IPMC input signal.

To determine the wave propagation profile with time and edge length, equation (6) is solved and results in the dimensionless presentation shown in figure 9. The gel head edge at which the wave is created has a width of 5 mm. The slider switch point position is adjusted at the middle of gel head and its width is set so that the duration time is 0.25% of each cycle.

Figure 10 shows the chemical wave profile as it reaches and leaves the contact point, which is. The cycle time of the wave depends on the malonic acid concentration in the reaction beginning, the cycle time in this work is set to 60 seconds. It results in t1=15 sec. and t2= 30 sec. the resultant voltage input pulses for one operating cycle is illustrated and then it is simulated with signal builder block inside the Simulink model.
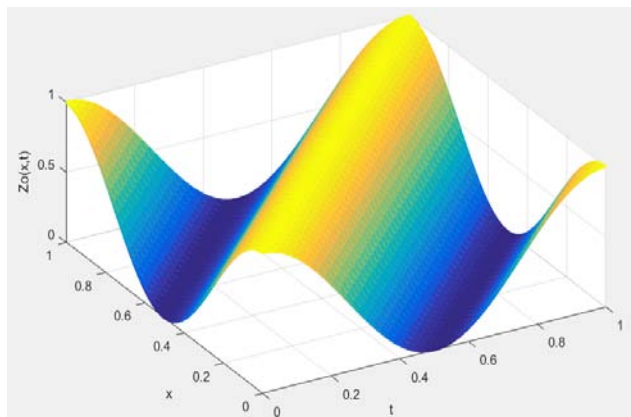
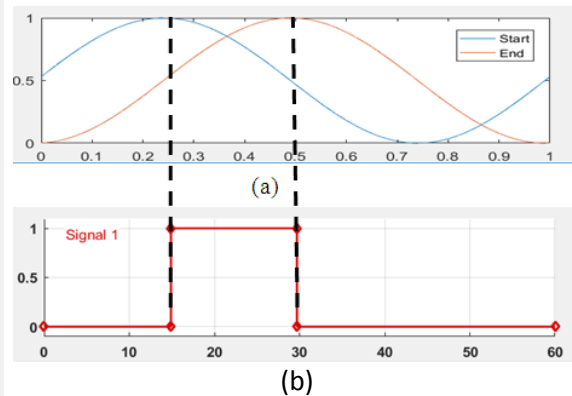**Figure 9.** Chemical wave propagation along the gel head edge.

Figure 10. (a) Wave profiles at signal start and end and (b) The resultant voltage signal for one cycle.

The previously estimated IPMC mathematical model is built on MATLAB Simulink as shown in figure 11 with the input voltage signal results from the previous stage. A pulse of voltage of 1 vols is given to the system simulation as an input signal at the previously determine times. The model is estimated for an IPMC strip deflection is adopted from [30], which addresses the IPMC deflection due to input voltage at no load at the tip. The transfer function parameters (a, b, c, d, e) are estimated using system identification toolbox with one zero and two poles to match the estimated model configuration. To estimate our actuator performance, the mathematical model is extended to find the resultant IPMC tip force and slider displacement relative to the input voltage signal. The model parameters are estimated based on the mechanical and electrical properties of the moving parts given in Table 1.
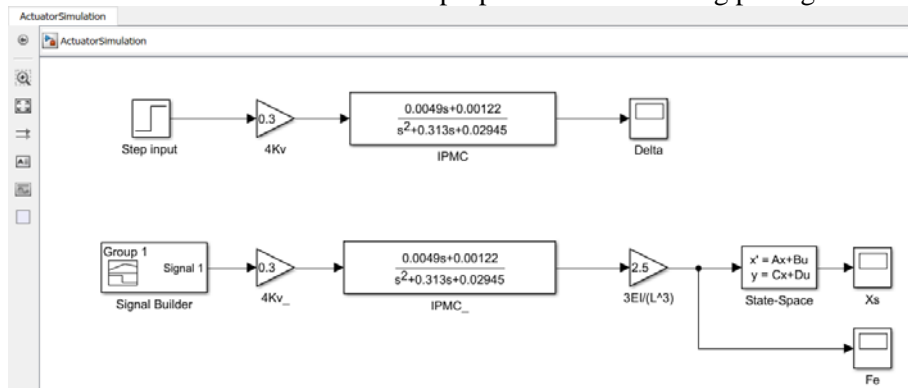
Figure 11. MATLAB Simulink model of the proposed actuator.

Table 1. Model mechanical parameters

Parameter	Value
Nafion Density (kg/m^3)	2100
Electrode Density (kg/m^3)	19300
$E\ (Pa)$	$8*10^7$
$B\ (m)$	0.000032
$L*w\ (m2)$	0.03*0.005
$m_s\ (kg)$	0.002
k_v	0.075
$k_{eq}(N/m)$	0.01
$D_{eq}(N.s/m)$	0.01

The model simulation was run on two steps, the first step was done to validate the estimated model on the adopted data using a step input signal of 3 volts and the step response is analyzed. Afterwards, the estimated model of the mechanical and electrical model parts is built combined with signal builder to simulate the resultant voltage signal to study the actuator performance criteria for one cycle, which are the slider displacement and actuator force.

The resultant step response of the identified model is shown in figure 12. It was analysed and found to have a good match with the original model step response. Then it was convenient to use the resultant voltage deflection transfer function given by equation (24);

$$\frac{\delta(s)}{V(s)} = \frac{0.3(0.0049s + 0.00122)}{s^2 + 0.313s + 0.02945} \tag{24}$$

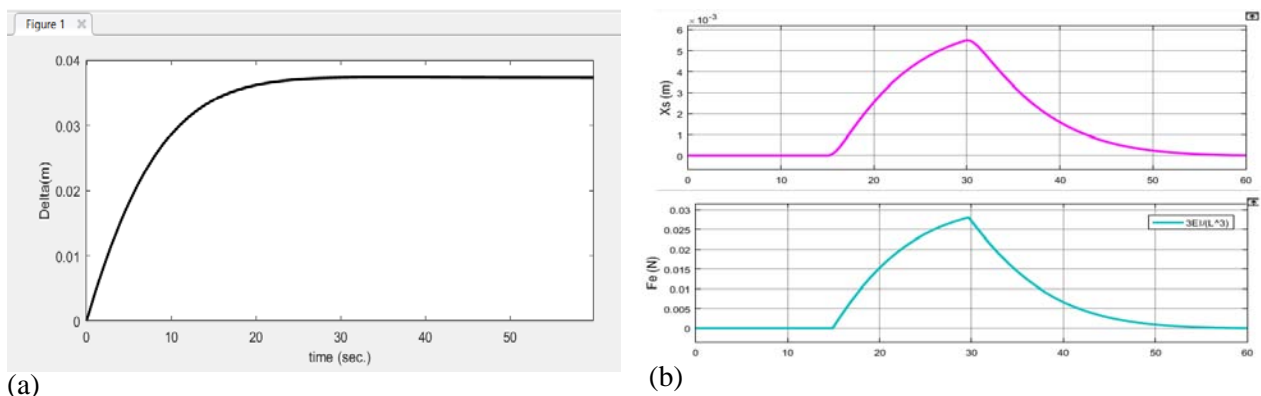(a)   (b)

Figure 12. (a) Unit step response of the IPMC tip deflection for step input 1 volt based on identified data. (b) Slider Displacement and and Actuator Force.

Based on the abovementioned results, it can be concluded that, for input signal of 1 volt for duration time of 15 seconds, the resultant actuator slider axial movement is 5 mm, and the maximum tip force is 0.028 N. These performance measurements result from one actuating module (one IPMC strip connected with gel head) illustrated in the design model.

6. Conclusion

Inspired by the four-step cycle of the natural sarcomere, this work presents an autonomous, hybrid material, single unitartificial sarcomere. The beating hydrogel head is powered by the BZ chemical reaction, the chemical wave propagation which is responsible for voltage signal creation is estimated based on the nature of the wave inside the gel. The IPMC strip is analysed by an electromechanical model to determine the proposed actuator characteristics. This work focused on the study of one operating cycle of one actuating module. The proposed design has the ability to repeat the cycle without any external signal because of cyclic nature of BZ reaction, which is considered a privilege enables the artificial actuators to act in natural behavior to improve their performance. The resultant actuation force is relatively small, so the mechanical design is proposed so that it has extendable configuration to add more modules in order to enhance the resultant response, actuation force and displacement.

References
[1]   Nomura M, Volkenburgh E and Mizunami M 2016 Bioinspired Actuators and Sensors *Cambridge University Press*.
[2]   Abdelwahab S 2015 Design and Development of a Motion Control System Based on Human Like Actuator and IP *Ain Shams University*.

[3]   Peng C, Yin Y, Hong H, Zhang J, and Chen X 2017 Bio-inspired design methodology of sensor-actuator-structure integrated system for artificial muscle using SMA *Procedia CIRP* **65** p 299.

[4]   Hilber W 2016 Stimulus-active polymer actuators for next-generation microfluidic devices *Appl. Phys. A Mater. Sci. Process* **122**(8) p 1-39.

[5]   Bar-cohen Y 2002 Electroactive Polymers as Artificial Muscles: A Review Introduction **39**(6).

[6]   Tolbah F, Abdelhameed M, Awad M and Abdelwahab S 2014 Modelling and simulation of a new bioinspired muscle actuator *5th Int. Work. Res. Educ. Mechatronics.*

[7]   Seeley C, Rod, Russo, Andy, Regan, Jennifer and VanPutte 2014 Anatomy & Physiology *McGraw-Hill.*

[8]   Williams W 2011 Huxley's model of muscle contraction with compliance *Journal of Elasticity* **105**(1–2) p 365–380.

[9]   Jovanovic K, Vranic J and Miljkovic N 2015 Hill's and Huxley's muscle models - tools for simulations in biomechanics *Serbian J. Electr. Eng* **12**(1) p 53–67.

[10]   Lymn R and Taylor E 1971 Mechanism of Adenosine Triphosphate Hydrolysis by Actomyosin *Biochemistry* **10**(25) p 4617–24.

[11]   Chen J, Zhang X, Lin S, Wang H and Gu L 2015 Multiscale modeling of skeletal muscle active contraction in relation to mechanochemical coupling of molecular motors *Micromachines* **6**(7) p 902–14.

[12]   Chen J, Zhang X and Wang H 2015 Research on Biomechanical Model of Muscle Fiber Based on Four-State Operating Mechanism of Molecular Motors *IEEE –NEMS* p 529–32.

[13]   Kull F and Endow S 2013 Force generation by kinesin and myosin cytoskeletal motor proteins *Journal of Cell Science* **126** (1) p 9–19.

[14]   Calvert P 2008 Gel Sensors and Actuators *MRS Bull* **33**(3) p 207–12.

[15]   Ballhause D and Wallmersperger T 2008 Coupled chemo-electro-mechanical finite element simulation of hydrogels : I Chemical stimulation (*IOP Science Smart Mater. Struct* p 1-10.

[16]   Yoshida R, Kokufuta E and Yamaguchi T 1999 Beating polymer gels coupled with a nonlinear chemical reaction Beating polymer gels coupled with a nonlinear chemical reaction *Choas* **9**(2) p 260-66.

[17]   Yoshida R and Ueki T 2014 Evolution of self-oscillating polymer gels as autonomous polymer systems (*Nature Publishing Group* **6** p 1–14.

[18]   Maeda S, Hashimoto S and Yoshida R 2004 Design of chemo-mechanical actuator using self-oscillating gel *IEEE International Conference on Robotics and Biomimetics* p 474–79.

[19]   Yashin V, Levitan S and Balazs A 2015 Modeling the entrainment of self-oscillating gels to periodic mechanical deformation *Chaos: An Interdisciplinary Journal of Nonlinear Science* **25**(6) p 1-9.

[20]   Vokoun D, He Q, Heller L, Yu M and Dai Z 2015 Modeling of IPMC Cantilever' Displacements and Blocking Forces *J. Bionic Eng* **12**(1) p 142–51.

[21]   Kazem B and Khawwaf J 2016 Estimation Bending Deflection in an Ionic Polymer Metal Composite (IPMC) Using Artificial Neural Network Model (*Jordan Journal of Mechanical and Industrial Engineering* **10**(2) p 123–31.

[22]   Kim K *et al.* 2016 Electromechanically Active Polymers *London UK- Springer.*

[23]   Ruiz S 2013 3D Modeling and Design Optimization of Rod Shaped Ionic Polymer Metal Composite Actuator *University of Nevada, Las Vegas.*

[24]   Yashin V and Balazs A 2007 Theoretical and computational modeling of self-oscillating polymer gels Theoretical and computational modeling of self-oscillating polymer gels *Journal of Chemical Physics* **126** p 1-17.

[25]   Moeinkhah H, Rezaeepazhand J and Akbarzadeh A 2013 Analytical dynamic modeling of a cantilever IPMC actuator based on a distributed electrical circuit *Smart Mater. Struct.* **22**(5) p 1-10.

[26]   Wang Z, He B, Liu X, and Wang Q 2017 Development and modeling of a new ionogel based actuator (*J. Intell. Mater. Syst. Struct.* **28**(15) p 2036–50.

[27]   Dougal R, Gao L and Liu S 2004 Ultracapacitor model with automatic order selection and capacity scaling for dynamic system simulation (*J. Power Sources* **126**(1–2) p 250–57.

[28]   Shi L, Guo S and Asaka K 2012 Modeling and experiments of IPMC actuators for the position precision of underwater legged microrobots *IEEE Int. Conf. Autom. Logist. ICAL* p. 415–20.

[29]   Gong Y, Fan J, Tang C and Tsui C 2011 Numerical simulation of dynamic electro-mechanical response of ionic polymer-metal composites *J. Bionic Eng* **8**(3) p 263–72.

[30]   Gutta S, Trabia M and Yim W 2007 Modeling of ionic polymer metal composite actuator *ASME International Mechanical Engineering Congress and Exposition.*